

# A Y-AXIS SOI-MEMS GYROSCOPE WITH A ZIGZAG-SHAPED Z-ELECTRODE SUPPORTED BY THREE-DIMENSIONALLY-INTERSECTED Z-BEAMS

T. Akashi, Y. Omura, H. Funabashi, M. Fujiyoshi, Y. Nonomura, and Y. Hata  
Toyota Central R&D Labs., Inc., Nagakute, Aichi, JAPAN

## ABSTRACT

The present paper describes a novel y-axis SOI-MEMS gyroscope with a zigzag-shaped Z-electrode (ZSZ) for detecting the roll rate. The proposed gyroscope is three-dimensionally (3D) structured by fabricating double-sided bulk silicon layers of an SOI substrate. The ZSZ supported by 3D-intersected Z-beams has a parallel-plate structure for differentially sensing z-directional capacitive changes. As a proof mass, it is electrostatically vibrated by a 200- $\mu\text{m}$ -thick bottom-layer drive comb. The fabricated gyroscope was evaluated at 100 Pa. The measured sensitivity was 62.3 aF/( $^{\circ}$ /s) with a nonlinearity of less than 0.36% for a full scale of 360 $^{\circ}$ /s. The test results demonstrate that the proposed y-axis gyroscope with the structurally differential ZSZ works for detecting the roll rate.

## KEYWORDS

SOI-MEMS, gyroscope, zigzag-shaped Z-electrode, Z-beam, differential detection, roll rate

## INTRODUCTION

Automobiles are a major application of MEMS inertial sensors. Many sensors have been used to improve driving safety. In particular, for vehicle stability control, an inertial sensor composed of an accelerometer and a gyroscope has been used to detect both the in-plane two-axis acceleration and the yaw rate. Since the sensor is used for automotive applications, high reliability and long-term stability against temperature changes and mechanical shock vibrations are required, unlike in consumer applications. For a more advanced vehicle control system, in addition to perpendicular-axis gyroscopes, lateral-axis gyroscopes with high resolution will be required in the future.

Recently, lateral-axis SOI-MEMS gyroscopes have been reported [1-3]. They used vertical combs for sensing the z-directional displacement as a capacitive change. Differential detection is required for precisely sensing the roll rate. Therefore, for z-directional differential detection, previous gyroscopes [2-3] required not only comb fingers with different heights but also a pair of sensor elements as a tuning-fork structure for canceling in-phase acceleration. Moreover, the tuning-fork gyroscopes were required to maintain mass balance of the two elements for improving sensor performance.

In contrast, for z-directional differential capacitive detection, we first reported a zigzag-shaped Z-electrode (ZSZ), which was applied to an SOI three-axis accelerometer [4], as a gap-changing parallel-plate capacitor. The ZSZ was structured using double-sided single-crystal silicon layers of an SOI substrate with high reliability and stability. In our previous work, the ZSZ succeeded in statically sensing z-directional differential capacitive changes, and our three-axis accelerometer

demonstrated good sensor performance with low cross-axis sensitivity and nonlinearity.

In this work, to detect the roll rate, we propose a novel y-axis SOI-MEMS gyroscope with a structurally differential ZSZ supported by three-dimensionally (3D) intersected Z-beams. The proposed gyroscope has a 3D structure, and the ZSZ is electrostatically vibrated in the x-axis direction using an extremely thick bottom-layer drive comb.

## GYROSCOPE DESIGN

### 3D Structure and Working Principle

Figure 1 illustrates the proposed y-axis gyroscope. The gyroscope is structured using both top and bottom bulk silicon layers of an SOI substrate. Typically, a thick bottom handle layer is used for device formation. This means that the gyroscope is 3D structured.

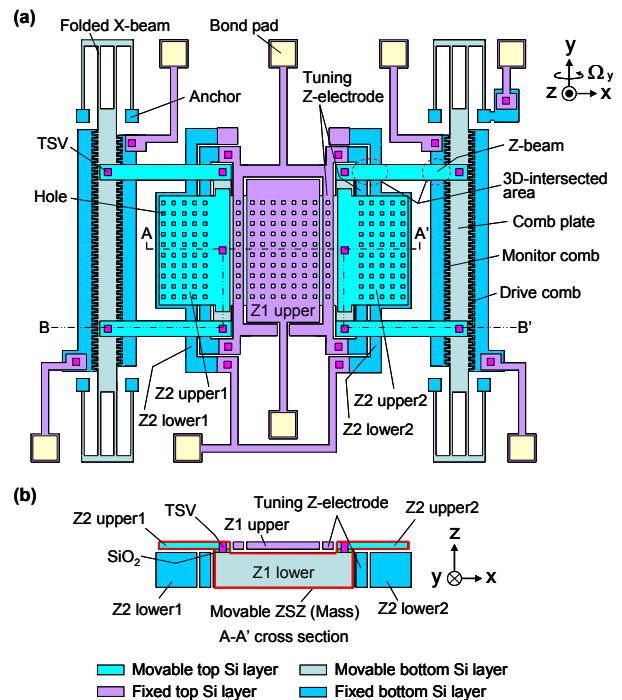


Figure 1: Schematic diagram of the y-axis SOI-MEMS gyroscope with the ZSZ supported by the 3D-intersected Z-beams: (a) top view and (b) cross-sectional view along the A-A' line shown in (a).

The movable ZSZ consists of the Z1-lower, Z2-upper1, and Z2-upper2 electrodes, as shown in Figure 1(b). Those electrodes are mechanically and electrically connected via an SiO<sub>2</sub> layer and a through-silicon via (TSV), respectively. Moreover, the ZSZ is mechanically and electrically connected to one end of four straight Z-beams. This means that the ZSZ is supported by those Z-beams formed on the top layer. Since the gyroscope structure is formed on double-sided silicon layers, the Z-beams 3D intersect the

bottom-layer structures such as the Z2-lower1 and Z2-lower2 electrodes. The other ends of the Z-beams are connected to a bottom-layer comb plate composed of movable monitor and drive combs. The comb plate is supported by bottom-layer folded X-beams, one end of which is connected to an anchor. The combs and X-beams are extremely thick because they are structured on the bottom handle layer. This configuration for increasing the z-directional stiffness allows the suppression of quadrature error caused by x-directional vibration.

In the proposed gyroscope, the ZSZ works as both a proof mass and a z-directional differential parallel-plate capacitor. Due to the straight and folded beam configuration, the ZSZ connected to the comb plate via the Z-beams has high axial independence. This means the ZSZ can be vibrated without mechanical coupling in the x-axis direction in the drive mode and in the z-axis direction in the sense mode. When an angular rate is applied about the y axis of the gyroscope, a Coriolis force is induced in the z-axis direction, and the ZSZ is also vibrated in the z-axis direction. When the ZSZ moves in the z-axis direction, the gap between the Z1 electrodes decreases, whereas the two gaps between the Z2 electrodes increase [4]. This means the ZSZ has a differential parallel-plate structure.

Compared with a Z-beam fabricated by thinning, this Z-beam can be expected to easily control the z-directional resonant frequency because its thickness is equal to the top-layer thickness. In addition, such a z-directional resonant frequency can be tuned using a tuning Z-electrode formed on both layers for an improvement in sensitivity.

### Design of Sensor Element

The gyroscope structure was first designed using analytical equations. In this work, the resonant frequencies in the drive and sense modes were set to be around 6 kHz, and the applied angular rate was set to be in the range of  $\pm 180^\circ/\text{s}$ .

When the roll rate  $\Omega_y$  is applied around the y axis of the gyroscope, the z-directional displacement  $z$  can be expressed as

$$z = \frac{x \Omega_y Q_{stdz}}{\pi f_z} \quad (1)$$

where  $x$  is the x-directional vibration amplitude of the ZSZ,  $f_z$  is the z-directional resonant frequency, and  $Q_{stdz}$  is the standardized quality factor, which is given as

$$Q_{stdz} = \frac{1}{\sqrt{\left\{ (1-R_d) - \frac{1}{1-R_d} \right\}^2 + \left( \frac{1}{Q_z} \right)^2}} \quad (2)$$

$$R_d = \frac{f_x - f_z}{f_x} \quad (3)$$

where  $R_d$  is the detuning ratio,  $Q_z$  is the quality factor in the z-axis sensing direction, and  $f_x$  is the x-directional resonant frequency.

The resonant frequency  $f_z$  is tuned by applying a DC voltage  $V_{dc}$  to the tuning Z-electrode. The tuned z-directional resonant frequency  $f_z'$  is expressed as

$$f_z' = \sqrt{f_z^2 - \frac{\epsilon_0 S V_{dc}^2}{2\pi^2 m d_0^3}} \quad (4)$$

where  $\epsilon_0$  is the permittivity in a vacuum,  $S$  is the area of the

tuning Z-electrode,  $m$  is the vibrating mass, and  $d_0$  is the gap between the tuning Z-electrode and the vibrating mass.

Regarding the conversion from voltage into capacitance, when both the feedback capacitance  $C_f$  and the reference voltage  $V_R$  of a preamplifier are already given, the capacitive change  $\Delta C$  corresponding to the measured voltage change  $\Delta V$  can be shown as

$$\Delta C = \frac{\Delta V}{V_R} C_f \quad (5)$$

For the sensor element design,  $R_d$  was set to -1.5%. Then,  $Q_z$  was set to 800, which has less impact on the sensitivity proportional to the z-directional displacement  $z$  because  $R_d$  is relatively large. The gyroscope structure was designed to obtain a differential capacitive change of 40 aF/( $^\circ/\text{s}$ ) for a 1- $\mu\text{m}$  vibration amplitude. In addition, based on Equation (4), the tuning Z-electrode structure was designed for tuning an  $R_d$  of -1.5% to match the modes by applying about 15 V.

Next, a finite element method (FEM) simulation was performed to design  $R_d$  using the ANSYS<sup>TM</sup> simulation software. Figure 2 shows the FEM modal analyses of the proposed gyroscope. For quick modeling, the gyroscope structure was simplified. In this case, the structure of the monitor and drive combs was simplified; namely, a mass equivalent to such combs was added to the comb plate. Based on the simulation, the first mode was designed to be the drive mode, in which the ZSZ vibrates in the x-axis direction, whereas the second mode was designed to be the sense mode, in which the ZSZ vibrates in the z-axis direction.

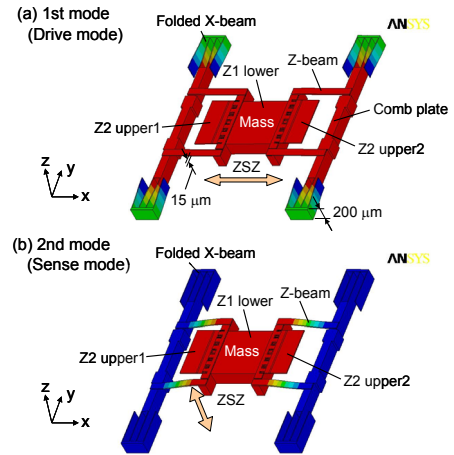


Figure 2: Modal analyses by ANSYS<sup>TM</sup> FEM simulation: (a) drive mode and (b) sense mode.

## FABRICATION

### Process

Figure 3 illustrates the fabrication process flow for the proposed y-axis gyroscope. The starting material was an SOI wafer composed of a 15- $\mu\text{m}$ -thick top silicon layer, a 2- $\mu\text{m}$ -thick buried oxide layer, and a 200- $\mu\text{m}$ -thick bottom silicon layer. Each process step is explained below.

In step (1), an undoped silicate glass (USG) was first deposited on the top layer. Next, a USG mask was patterned for poly-Si TSVs. Then, deep reactive ion etching (DRIE) of the top layer, refilling with doped poly-Si, and dry etchbacking of the deposited film were

performed. These processes produced the poly-Si TSVs. Subsequently, for the DRIE of the bottom layer, a bottom SiO<sub>2</sub> mask was patterned. In step (2), the USG mask was again patterned for fabricating the top structure. In step (3), Al-Si-Cu was sputtered and patterned on the top layer. In steps (4) and (5), the double-sided DRIE was implemented to form the top and bottom structures. Finally, the structure was released by HF vapor sacrificial etching in step (6).

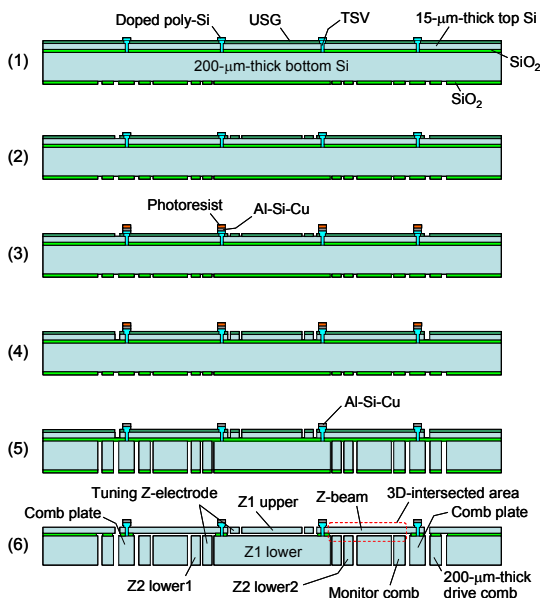


Figure 3: Fabrication process flow for the gyroscope: cross-sectional view along the B-B' line in Figure 1(a).

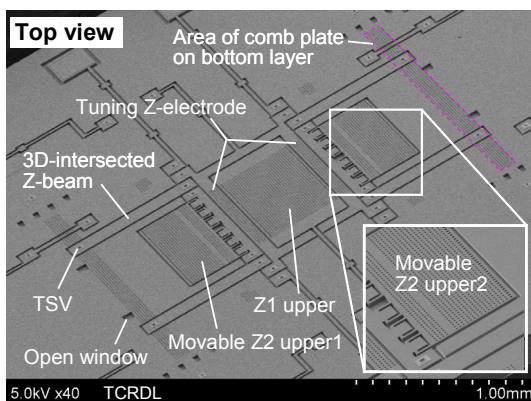


Figure 4: Top view of the fabricated gyroscope with the SZS supported by the 3D-intersected Z-beams.

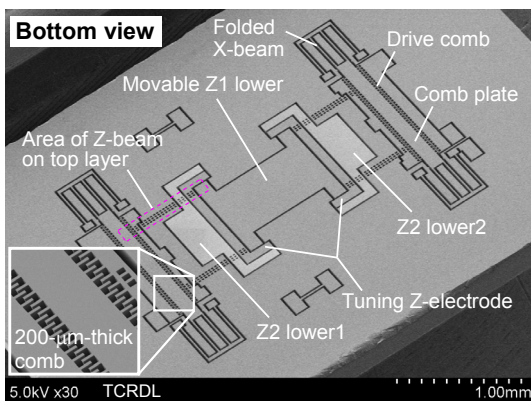


Figure 5: Bottom view of the fabricated gyroscope with the SZS, 200-μm-thick X-beam, and drive comb.

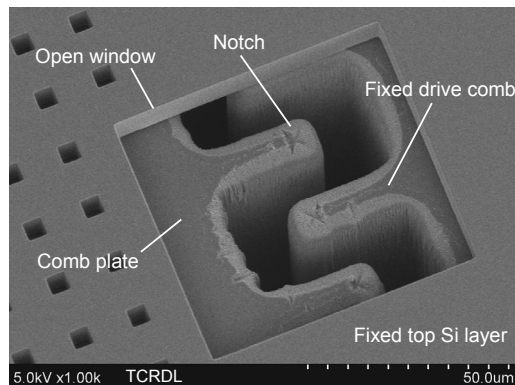


Figure 6: Large notch formation, which was observed through an open window on the top silicon layer.

## Fabrication Results

Based on the above-mentioned process steps, the gyroscope with a 3D structure was successfully fabricated. Figures 4 and 5 are SEM pictures showing the top and bottom views of the fabricated gyroscope. In Figure 4, the 3D-intersected straight Z-beams, fixed Z1-upper, and movable Z2-upper electrodes were formed on the 15-μm-thick top silicon layer. The area surrounded by the dotted line indicates the position of the comb plate formed on the bottom layer. In Figure 5, on the other hand, the comb plate, drive comb, folded X-beams, movable Z1-lower, and fixed Z2-lower electrodes were formed on a 200-μm-thick bottom silicon layer.

In this work, a comb structure with a gap of 10 μm was fabricated. For the successful fabrication of such an extremely thick comb structure, bridge formation caused by silicon residues must be avoided [5]. Therefore, a fan-shaped compensation pattern was added to the comb tips close to the position where the comb gap remarkably changes. This pattern prevented the bridge formation. However, the large notch formation degraded the comb shape close to the etch-stop SiO<sub>2</sub> layer, as shown in Figure 6. This problem could be improved by changing the DRIE conditions.

## EXPERIMENTAL RESULTS

### Experimental Setup

The gyroscope characteristics were evaluated by using a dedicated vacuum chamber incorporating a turntable. Figure 7 illustrates the experimental setup for the evaluation. The pressure inside the chamber was manually controlled using three kinds of valves, and it was precisely monitored using a ceramic capacitance manometer. The turntable was rotated in the vacuum by a servo motor outside the chamber. Even though the turntable is rotated, the pressure is stably controllable down to 30 Pa.

The fabricated gyroscope and its preamplifier for a capacitance-to-voltage converter were mounted close to each other on the same ceramic substrate in a metal can package. The test sensor block assembling the gyro package was placed on an L-shaped jig for rotating the gyroscope around the y axis. The resonant frequency and sensor output were electrically measured using a lock-in amplifier via the preamplifier without amplification. Based on Equation (5), the vibration amplitude was obtained by measuring the output voltage of the monitor combs.

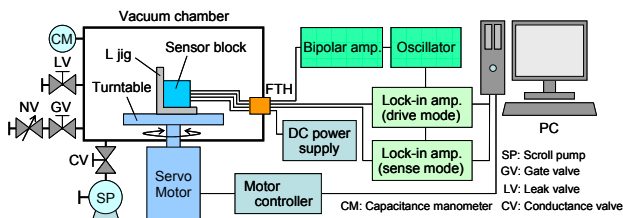


Figure 7: Experimental setup for the gyroscope evaluation.

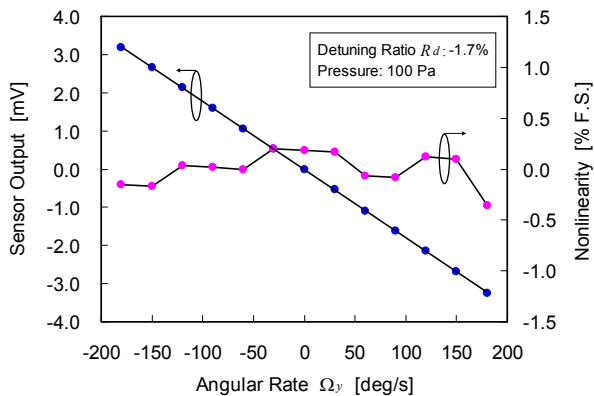


Figure 8: Measured sensor output characteristics of the fabricated gyroscope (pressure: 100 Pa).

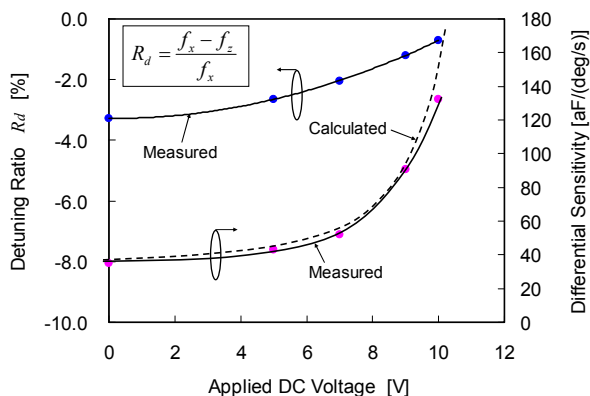


Figure 9: Measured frequency tuning characteristics of the fabricated gyroscope (pressure: 100 Pa).

### Dynamic and Sensor Output Characteristics

At first, the resonant frequencies in the drive and sense modes were measured at 100 Pa. The values of  $f_x$  and  $f_z$  were 5787 and 5888 Hz, respectively. The detuning ratio  $R_d$  was calculated as -1.7%. Moreover, the measured quality factors in the drive and sense modes were 904 and 755, respectively.

Next, the sensor output characteristics at 100 Pa were evaluated using the turntable in Figure 7. In this experiment, the feedback capacitance  $C_f$  and reference voltage  $V_R$  were 1.06 pF and 304 mV, respectively. Figure 8 shows the measured differential sensor output. The figure shows that the scale factor was  $-17.9 \mu\text{V}/(^{\circ}/\text{s})$ , which corresponded to a sensitivity of  $62.3 \text{ aF}/(^{\circ}/\text{s})$  based on Equation (5). The measured value agrees well with the calculated sensitivity of  $67.8 \text{ aF}/(^{\circ}/\text{s})$  for a  $1.7\text{-}\mu\text{m}$  amplitude. In addition, a nonlinearity of less than 0.36% for a full scale of  $360^{\circ}/\text{s}$  was experimentally obtained.

### Frequency Tuning Characteristics

Figure 9 shows the frequency tuning characteristics.

In this experiment, a gyroscope with a detuning ratio  $R_d$  of -3.3% was tested. As the DC voltage applied to the tuning Z-electrode increased, only the z-directional resonant frequency decreased. Consequently, as the detuning ratio  $R_d$  increased, the measured sensitivity improved and reached  $132 \text{ aF}/(^{\circ}/\text{s})$ , which is in good agreement with the calculated sensitivity indicated by the dotted line in the figure. It was experimentally confirmed that the tuning Z-electrode can change the detuning ratio  $R_d$  by 2.6% and can improve the sensitivity. These experimental results demonstrate that the fabricated tuning Z-electrode works properly.

## CONCLUSION

A y-axis SOI-MEMS gyroscope with a structurally differential ZSZ was presented to differentially detect the roll rate. The proposed gyroscope was 3D structured by fabricating double-sided silicon layers of an SOI substrate. The ZSZ supported by the 3D-intersected Z-beams was successfully vibrated by the bottom-layer drive comb. The gyroscope characteristics at 100 Pa showed that the measured sensitivity was  $62.3 \text{ aF}/(^{\circ}/\text{s})$  with a nonlinearity of less than 0.36% for a full scale of  $360^{\circ}/\text{s}$ , and the tuning Z-electrode worked well to improve the sensitivity. The experimental results demonstrated that the proposed y-axis gyroscope can detect the roll rate.

## REFERENCES

- [1] Z. Yang, C. Wang, G. Yan, Y. Hao, and G. Wu, "A Bulk Micromachined Lateral Axis Gyroscope with Vertical Sensing Comb Capacitors", in *Digest Tech. Papers Transducers '05 Conference*, Seoul, Korea, June 5-9, 2005, pp. 121-124.
- [2] Z.Y. Guo, Z.C. Yang, L.T. Lin, Q.C. Zhao, J. Cui, X.Z. Chi, and G.Z. Yan, "A Lateral-Axis Micromachined Tuning Fork Gyroscope with Novel Driving and Sensing Combs", in *Digest Tech. Papers Transducers '09 Conference*, Denver, CO, USA, June 21-25, 2009, pp. 288-291.
- [3] D. Maeda, H. Jeong, C. Takubo, M. Degawa, K. Yamanaka, M. Shoji, and Y. Goto, "Out-of-Plane Axis SOI MEMS Gyroscope with Initially Displaced Vertical Sensing Comb", in *Digest Tech. Papers Transducers '11 Conference*, Beijing, China, June 5-9, 2011, pp. 44-47.
- [4] M. Fujiyoshi, Y. Nonomura, H. Funabashi, Y. Omura, T. Akashi, Y. Hata, H. Yamada, and M. Esashi, "An SOI 3-Axis Accelerometer with a Zigzag-Shaped Z-Electrode for Differential Detection", in *Digest Tech. Papers Transducers '11 Conference*, Beijing, China, June 5-9, 2011, pp. 1010-1013.
- [5] H. Hata, Y. Nonomura, T. Akashi, H. Funabashi, M. Fujiyoshi, and Y. Omura, "A DRIE Compensation Mask Pattern for Fabricating an Extremely-Thick Comb Electrode", in *Digest Tech. Papers MEMS 2012 Conference*, Paris, France, January 29-February 2, 2012, pp. 208-211.

## CONTACT

\*T. Akashi, tel: +81-561-71-7171;  
t-akashi@mosk.tytlabs.co.jp